Proceedings of the
Annual Stability Conference
Structural Stability Research Council
Denver, Colorado, March 22-25, 2022

Three-dimensional frame buckling benchmark problems for direct analysis method in ANSI/AISC 360-16

Heera M Titus[1], S Arul Jayachandran[2]

Abstract
Direct Analysis Method (DAM) of ANSI/AISC 360-16 prescribes the use of a rigorous second-order analysis to account for initial imperfections, the spread of inelasticity, *P*-Δ, and *P*-δ effects accurately. The second-order analysis used in DAM should be verified against benchmark problems to ascertain whether it can accurately model all the second-order effects of a steel frame with reduced stiffness and notional loads. The benchmark problems available in the literature are primarily for frames with gravity loads acting through second-order displacements as the source of geometric nonlinearity. This paper identifies two lightly loaded structures where significant geometric nonlinearity occurs due to the behavior of individual elements and complexity in geometry. 3D frames can exhibit flexural, torsional, axial deformations and buckle through sway, non-sway, torsional and snap-through modes. For such structures, the position and direction of notional loads should be chosen accordingly to trigger the most undesirable displacements in the structure. Geometric nonlinear analyses are necessary when cable elements support the structure, even when the load is lateral. The inability of an analysis software verified against existing 1D and 2D benchmark problems in capturing the second-order effects of a cable-supported beam-column is illustrated in this study. The applicability of DAM on these structures is also discussed. Apart from software packages, a Total Lagrangian-based 3D finite element framework is also used to generate benchmark problems. These problems equip a designer to verify whether a second-order analysis software used for the DAM can accurately capture spatial behavior, flexural-torsional coupling, and different sources of nonlinearities consistently.

1. Introduction

Designers employing the Direct Analysis Method (DAM) are presented with a vexing problem of identifying an advanced method for the nonlinear analysis of steel frames. While the use of advanced analysis methods increases the modeling and computational effort, the design procedure gets exceedingly simplified as it omits the use of effective length factor and empirical column curves and identifies the effect of residual stresses, initial imperfections, and spread of inelasticity more consistently (Dierlein 2003; Geschwinder 2002; Shankar Nair 2007; Surovek and Ziemian 2005). DAM is generally applicable to all frames. It has no limits on the sidesway amplification

[1] Graduate Research Assistant, Indian Institute of Technology Madras, heer.titus@gmail.com
[2] Professor, Indian Institute of Technology Madras, arulsteel@gmail.com

factor. The components are designed for a higher moment than that of the Effective Length Method (ELM), which makes the design of beams and connections safe (Ingkiriwang and Far 2018; White and Hajjar 1997). DAM recognizes the specific advantage obtained by moving the effects of imperfections and stiffness reduction from the resistance side to the analysis side in the design equations. ANSI/AISC 360-16 explains how these are considered in the analysis by applying notional loads and stiffness reduction factors.

The design loads for DAM are highly sensitive to the accuracy of the geometric nonlinear analysis used. Hence, some benchmark problems are necessary to verify whether the second-order analysis can be used in DAM. Structures usually proposed as benchmark problems exhibit significant second-order effects. There are several references in the literature regarding the development of benchmark problems for use in stability design. These include moment frames, braced frames, gable frames, unsymmetric moment frames, unsymmetric braced frames, etc. (Chen and Toma 1994; Du et al. 2019; Surovek and White 2001; Toma et al. 1995; Vogel 1985; Ziemian and Ziemian 2021a; b).

While most of the benchmark problems are limited to two-dimensional behavior, it should be noted that accurate modeling of spatial behavior is essential for the design of any structure. A few 3D benchmark problems exist in the literature accounting for spatial behavior (Bai et al. 2019; Du et al. 2019; Liu et al. 2016; Teh 2004). They account for the reference line deformation and cross-sectional twists of the structural elements of the frame. Frames in which significant second-order effects develop primarily due to member twists need a different set of benchmark problems that account for accurate modeling of cross-sectional behavior in their analysis (Ziemian et al. 2018). While DAM is generally applicable to all frames, ANSI/AISC 360-16 suggests a notional load coefficient of 0.002 for frames that support gravity loads through nominally vertical structural elements. But, it is also specified that the notional load concept applies to all types of structures at points of intersection of members and points along members. The specifications in ANSI/AISC 360-16 are heavily rooted in the assumption that a gravity-loaded frame develops significant second-order effects only when the structure fails through a sway mode.

To push the boundaries of DAM (Chan et al. 2017; Dewobroto and Chendrawan 2018; Misiunaite and Juozapaitis 2015), one may need to agree that second-order effects may become significant even for lightly loaded systems. Other than the vertical load, which generates significant moments by out-of-plumbness and bowing of vertical elements, nonlinearities may arise in two ways: (*i*) When a torsional mode of frame system buckling can cause significant second-order effects, especially when the frame carry loads through inclined members (*ii*) When highly nonlinear structural elements like cables support the frame.

In all these cases, an analysis software verified using the two benchmark problems in ANSI/AISC 360-16 may still be incapable of capturing the nonlinearities. For a general frame, it is understood that the notional loads need to be identified by the designer from a linear buckling analysis. But, difficulties arise when there is a limit point, or the buckling loads are very close, making the system switch between two post-buckling paths. In such cases, notional loads which perturb the structure decide the path followed by the structure. Hence, the designer should determine the nature of perturbations, and the analysis tool should be able to do the branch switching. Section 3.1(Teh 2004) highlights how eluding the branch switching may underestimate the design force and design

bending moment in DAM. Similarly, the general perception about the lack of necessity of a nonlinear analysis when the structure is lightweight and loading is lateral is challenged by structures supported by cable elements. Cables stiffen under tension and sags under compression, making the structure highly nonlinear. It could be seen in Section 3.2 that even a widely used structural analysis software cannot capture cable nonlinearities accurately.

Capturing the spatial behavior needs a geometric nonlinear 3D analysis. Still, several nonlinear beam theories are incapable of accurately describing the deformed configuration with respect to the initial configuration, as they use truncated strain-displacement relations (Pai 2007, 2011). A geometrically exact beam theory may not be needed for all framed structures designed using DAM as the elements from the preliminary design are stiff enough to avoid large displacements. But, such restrictions regarding the flexibility of the individual elements should not be kept on benchmark problems. In that case, an advanced geometrically exact beam theory is needed to reveal their load-displacement responses. This paper summarizes an ongoing work at IIT Madras, a geometric nonlinear analysis framework that can model large beam-column displacements accurately. The analysis method used removes the problems due to shear locking, singularities during the description of large rotations and is appropriate to finite element modeling of flexible structures. The analysis method to be used in DAM need not be as accurate as the Total Lagrangian (TL) method in Section 2. Still, the generation of benchmark problems for verifying 3D beam elements should be based on methods capable of modeling large displacements.

2. Total Lagrangian formulation for 3D beam elements

This section describes a geometric nonlinear formulation that suits arbitrary elastic deformations and rigid body movements (Pai 2007, 2011). In a TL formulation, the deformed configuration is directly referenced to an inertial reference, and thus the strain-displacement relations fully account for rigid body displacements and elastic deformations. Hence, the complexity in formulating and solving the equilibrium equations gets reduced. Any large displacement formulation needs an exact description of the deformed configuration. In a 3D sense, spatial, sequential rotations are used to define the deformed shape exactly. Jaumann strains and stresses are used in the constitutive relation as they are independent of the rigid body movements in space. The relation between stress resultants and displacements is obtained using the principle of virtual displacements.

2.1 Kinematic description

Consider a 3D beam element whose undeformed and deformed shapes are shown in Fig. 1. *abc* is a fixed coordinate system, and *xyz* represents the undeformed coordinate system at the centroid of the cross-section, with *x*-axis representing the reference line (outward normal). ξηζ system represents the coordinate system of the deformed beam with ξ axis representing the deformed reference line and η and ζ axes representing the deformed *y* and *z* axes without considering warping deformations. i_a, i_b, i_c , i_x, i_y, i_z , i_1, i_2, and i_3 denote the unit vectors of *abc*, *xyz* and ξηζ system, respectively. *s* indicates the undeformed arc length along the *x* axis, and *u*, *v*, and *w* represent the displacement components of the centroid of the section with respect to *x*, *y*, and *z* axes, respectively.

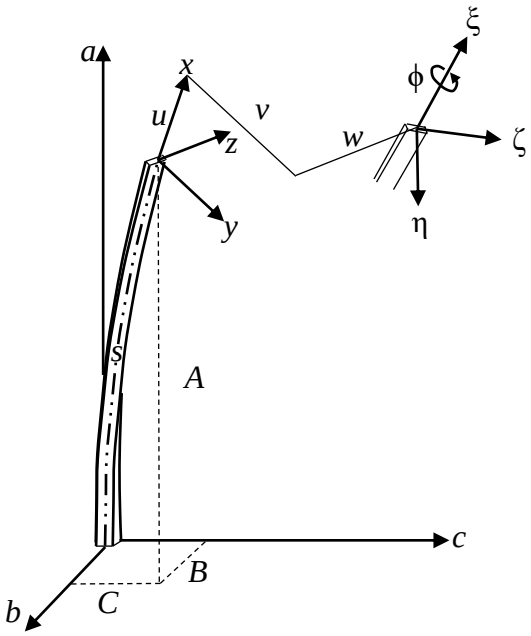

Figure 1: Three coordinate reference systems for modeling (Pai 2007)

The transformation matrices that relate the three coordinate systems are:

$$\begin{Bmatrix} i_x \\ i_y \\ i_z \end{Bmatrix} = \left[T^0\right] \begin{Bmatrix} i_a \\ i_b \\ i_c \end{Bmatrix}, \quad \begin{Bmatrix} i_1 \\ i_2 \\ i_3 \end{Bmatrix} = \left[T\right] \begin{Bmatrix} i_x \\ i_y \\ i_z \end{Bmatrix} \tag{1}$$

2.1.1 Initial transformation matrix [T^0]

If the undeformed position vector *R* is given as:

$$\bar{R} = A(s)i_a + B(s)i_b + C(s)i_c \tag{2}$$

$$i_x = \frac{d\bar{R}}{ds} = A'(s)i_a + B'(s)i_b + C'(s)i_c$$

Angles θ_{21}, $\theta_{22,}$ and θ_{23} are the direction cosine angles of *y*-axis with respect to *abc* system.

$$i_y = \cos\left(\theta_{21}\right)i_a + \cos\left(\theta_{22}\right)i_b + \cos\left(\theta_{23}\right)i_c \tag{3}$$

$$i_z = i_x \times i_y$$

Hence, the initial transformation matrix [T^0] is given by:

$$\left[T^0\right] = \begin{bmatrix} A' & B' & C' \\ \cos(\theta_{21}) & \cos(\theta_{22}) & \cos(\theta_{23}) \\ B'\cos(\theta_{23}) - C'\cos(\theta_{22}) & C'\cos(\theta_{21}) - A'\cos(\theta_{23}) & A'\cos(\theta_{22}) - B'\cos(\theta_{21}) \end{bmatrix} \tag{4}$$

$$\text{Also, } \frac{d}{ds}\begin{Bmatrix} i_x \\ i_y \\ i_z \end{Bmatrix} = [k]\begin{Bmatrix} i_x \\ i_y \\ i_z \end{Bmatrix} = \begin{bmatrix} 0 & k_3 & -k_2 \\ -k_3 & 0 & k_1 \\ k_2 & -k_1 & 0 \end{bmatrix}\begin{Bmatrix} i_x \\ i_y \\ i_z \end{Bmatrix} = \frac{\partial[T^0]}{\partial s}[T^0]^T \begin{Bmatrix} i_x \\ i_y \\ i_z \end{Bmatrix}$$

k_1, k_2, k_3 denote the initial curvatures of the undeformed configuration with respect to x, y, and z axes, respectively, and are functions of undeformed arc length s.

2.1.2 Transformation matrix of the deformed configuration [T]

Two successive Euler angles α and ϕ, and a vector n is used to describe the deformation of the beam element (Fig. 2). xyz is rotated by an angle α about n axis (perpendicular to x-axis) to an intermediate configuration $\xi y_1 z_1$. Then $\xi y_1 z_1$ is rotated by an angle ϕ about the ξ axis to obtain $\xi\eta\zeta$ system.

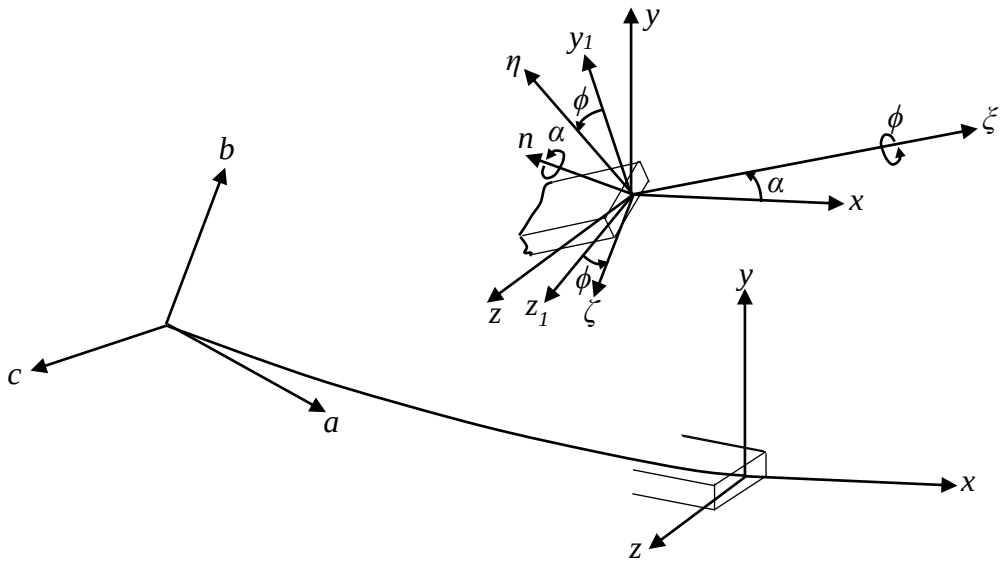

Figure 2: Description of deformed configuration (Pai 2007)

The components of transformation matrix [T] are expressed in terms of the displacements, displacement gradients, and initial curvatures as given below:

$$T_{11} = \frac{(1+u'-vk_3+wk_2)}{(1+e)}, \quad T_{12} = \frac{(v'+uk_3-wk_1)}{(1+e)}, \quad T_{13} = \frac{(w'-uk_2+vk_1)}{(1+e)} \tag{5}$$

$$T_{21} = -\cos(\phi)T_{12} - \sin(\phi)T_{13}, \quad T_{22} = \cos(\phi)\left(T_{11} + \frac{T_{13}^{\ 2}}{1+T_{11}}\right) - \sin(\phi)\left(\frac{T_{12}T_{13}}{1+T_{11}}\right)$$

$$T_{23} = \sin(\phi)\left(T_{11} + \frac{T_{12}^{\ 2}}{1+T_{11}}\right) - \cos(\phi)\left(\frac{T_{12}T_{13}}{1+T_{11}}\right), \quad T_{31} = sin(\phi)T_{12} - \cos(\phi)T_{13}$$

$$T_{32} = -\sin(\phi)\left(T_{11} + \frac{T_{13}^{\ 2}}{1+T_{11}}\right) - \cos(\phi)\left(\frac{T_{12}T_{13}}{1+T_{11}}\right), T_{33} = \cos(\phi)\left(T_{11} + \frac{T_{12}^{\ 2}}{1+T_{11}}\right) + \sin(\phi)\left(\frac{T_{12}T_{13}}{1+T_{11}}\right)$$

Also, $$\frac{d}{ds}\begin{Bmatrix} i_1 \\ i_2 \\ i_3 \end{Bmatrix} = [K]\begin{Bmatrix} i_1 \\ i_2 \\ i_3 \end{Bmatrix} = \begin{bmatrix} 0 & \rho_3 & -\rho_2 \\ -\rho_3 & 0 & \rho_1 \\ \rho_2 & -\rho_1 & 0 \end{bmatrix}\begin{Bmatrix} i_1 \\ i_2 \\ i_3 \end{Bmatrix} = \frac{\partial[T]}{\partial s}\begin{Bmatrix} i_x \\ i_y \\ i_z \end{Bmatrix} + [T]\frac{d}{ds}\begin{Bmatrix} i_x \\ i_y \\ i_z \end{Bmatrix}$$

$$[K] = [T]'[T]^T + [T][k][T]^T = ([K][T] - [T][k])[T]^T + [T][k][T]^T$$

ρ_1, ρ_2, ρ_3 denote the curvatures of the deformed configuration with respect to ξ, η, and ζ axes respectively.

2.2 Equilibrium equations

After describing the final configuration using deformations, slopes, and curvatures, the total strain energy of the system is represented using virtual displacements and virtual rotations. The principle of stationary potential energy is used to obtain the governing equation of the beam element.

$$\delta(\Pi - W) = 0 \tag{6}$$

The dot product of the variation of unit vector in deformed axes and the unit vector perpendicular to it gives the virtual rotation about the axis perpendicular to the plane of the axes considered. These rotations ($\delta\theta_i$, $for\ i = 1,2,3$) are infinitesimal and hence assumed vectorial and mutually independent. Then,

$$\begin{Bmatrix} \delta e \\ (1+e)\delta\theta_3 \\ -(1+e)\delta\theta_2 \end{Bmatrix} = [T]\begin{Bmatrix} \delta u' \\ \delta v' \\ \delta w' \end{Bmatrix} - [T][k]\begin{Bmatrix} \delta u \\ \delta v \\ \delta w \end{Bmatrix} \tag{7}$$

Variation of curvatures with respect to deformed axes are:

$$\begin{Bmatrix} \delta\rho_1 \\ \delta\rho_2 \\ \delta\rho_3 \end{Bmatrix} = \begin{Bmatrix} (\delta\theta_1)' \\ (\delta\theta_2)' \\ (\delta\theta_3)' \end{Bmatrix} - [k]\begin{Bmatrix} \delta\theta_1 \\ \delta\theta_2 \\ \delta\theta_3 \end{Bmatrix} \tag{8}$$

Strain measures are defined with respect to the deformed coordinate systems ξ, η, and ζ. The total displacement will have rigid body displacements and elastic deformations. The elastic deformation of the system is calculated by subtracting components of rigid body displacements from total displacement. The strains are given by:

$$B_{11} = e + z\bar{\rho}_2 - y\bar{\rho}_3, \quad B_{12} = -\frac{1}{2}z\bar{\rho}_1, \quad B_{13} = \frac{1}{2}z\bar{\rho}_1 \tag{9}$$
$$B_{22} = B_{23} = B_{33} = 0, \quad \bar{\rho}_i = \rho_i - k_i$$

where k_i is the initial curvature of the beam. If J_{ij} represents the stresses, the total variation of potential energy is:

$$\int_0^L \begin{pmatrix} -\left[\left(\{F_1,F_2,F_3\}[T]\right)'+\{F_1,F_2,F_3\}[T][k]\right]\{\delta u,\delta v,\delta w\}^T \\ -(M_1'+M_3\rho_2-M_2\rho_3+q_4)\delta\theta_1-\{q_1,q_2,q_3\}\{\delta u,\delta v,\delta w\}^T \end{pmatrix}.ds + \left[M_1\delta\theta_1+M_2\delta\theta_2+M_3\delta\theta_3+\{F_1,F_2,F_3\}[T]\{\delta u,\delta v,\delta w\}^T\right]_0^L = 0 \quad (10)$$

where,

$$F_1=\int_A J_{11}.dA,\quad M_1=\int_A\left(J_{13}y-J_{12}z\right).dA,\quad M_2=\int_A\left(J_{11}z\right).dA,\quad M_3=\int_A\left(-J_{11}y\right).dA,$$

$$F_2=\frac{1}{1+e}\left(-M_3'-M_2\rho_1+M_1\rho_2-q_6\right),\quad F_3=\frac{1}{1+e}\left(M_2'-M_3\rho_1+M_1\rho_3+q_5\right)$$

q_1, q_2, q_3 are distributed loads along *x, y,* and *z axes, and* q_4, q_5, q_6 are distributed moments along ξ, η, and ζ axes, respectively. Setting the coefficients of δ*u*, δ*v*, δ*w*, and $\delta\theta_1$ to zero yields the following governing equations which are entirely dependent on *u, v, w,* T_{21}, and T_{23}.

$$[k][T]^T\begin{Bmatrix}F_1\\F_2\\F_3\end{Bmatrix}-\frac{\partial}{\partial s}\left([T]^T\begin{Bmatrix}F_1\\F_2\\F_3\end{Bmatrix}\right)=\begin{Bmatrix}q_1\\q_2\\q_3\end{Bmatrix} \quad (11)$$

2.3 Finite element formulation

The weak form of the system is given as:

$$\delta\Pi=\int_0^L\{\delta\psi\}^T[D]\{\psi\}.ds \quad (12)$$

where

$$[D]=\begin{bmatrix}EA&0&0&0\\0&GI_1&0&0\\0&0&EI_2&0\\0&0&0&EI_3\end{bmatrix},\{\delta\psi\}=[\Psi]\{\delta U\},\Psi_{ij}=\frac{\partial\psi_i}{\partial U_j},\{U\}=[\partial N]\{q^{(i)}\}=[\partial][N]\{q^{(i)}\} \quad (13)$$

where [*N*] is a 5×16 matrix of shape functions of Hermite cubic polynomials and linear polynomials, and [∂] is a 13×5 matrix of differential operators.

For a two noded beam element,

$$\{q^{(i)}\}=\left\{u_j,v_j,w_j,u'_j,v'_j,w'_j,T_{21_j},T_{23_j},u_k,v_k,w_k,u'_k,v'_k,w'_k,T_{21_k},T_{23_k}\right\}^T \quad (14)$$

For a structure discretized into n_e elements with element length $L_i = L/n_e$,

$$\delta\Pi=\{\delta q\}^T[K]\{q\}=\sum_{i=1}^{n_e}\left\{\delta q^{(i)}\right\}^T\left[k^{(i)}\right]\left\{q^{(i)}\right\} \quad (15)$$

where $\left[k^{(i)}\right]\left\{q^{(i)}\right\} = \int_{L_i} \left[\partial N\right]^T \left[\Psi\right]^T [D]\{\psi\}.ds$

The global nodal load vector $\{R\}$ is obtained using:-

$$\delta W = \sum_{i=1}^{n_e} \left\{\delta q^{(i)}\right\}^T \left\{R^{(i)}\right\} = \left\{\delta q\right\}^T \left\{R\right\} \tag{16}$$

The equations of equilibrium in matrix form are:

$$\left[K\right]\left\{q\right\} = \{R\} \tag{17}$$

The above system of equations is solved using incremental-iterative solutions based on arc-length methods. This TL formulation (Pai 2011) eliminates singularity and shear locking problems encountered in analyzing flexible beams or large displacement problems. Hence, this method is suggested to generate benchmark problems to verify the capabilities of a second-order analysis method. This method is highly accurate but rigorous to be used in the design using DAM. Still, a nonlinear method or software verified against benchmark problems generated using this formulation will have enough capabilities to capture the complexities in behavior and sources of nonlinearity in a structure.

3. Benchmark problems

A set of calibration problems are defined for the designers to assess the capabilities of a geometric nonlinear analysis computer program to identify the sources of nonlinearity in a structural system. Two examples have been proposed. A hexagonal frame (Teh 2004) is adopted to establish the effect of one notional load and a pair of equal and opposite notional loads on the stability of the frame—the structure switches from a translational mode to a rotational mode in the post-buckling region. In order to identify the highly nonlinear behavior of a beam-cable system, a 2D beam-column supported by a single set of cables is provided. Even though the structure resists only lateral load and has no self-weight, it could be seen that the behavior is highly nonlinear under large displacements and structural analysis software like SAP2000 cannot accurately capture the nonlinearity.

3.1 Hexagonal space frame

This example may be used as a benchmark problem to ascertain the capabilities of a second-order analysis software for DAM under the following conditions:

(*i*) When the frame supports gravity load through inclined structural elements

(*ii*) When the frame has coincidental or nearly close post-buckling paths, and there is a chance of switching between them

A 3D hexagonal dome is provided to detect the capabilities of a second-order analysis method in identifying the branch switching of a structure between different post-buckling paths. While the second-order analysis chosen for DAM must satisfy the requirements given in Section C1 of ANSI/AISC 360-16 (2016), the section does not define the clauses when the frame switches between the post-buckling paths.

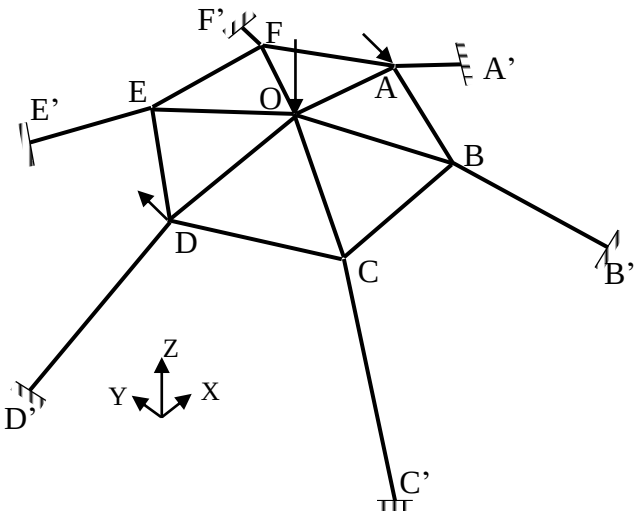

Figure 3: Hexagonal frame (Teh 2004)

Table 1: Geometry of the frame in Fig. 3

Coordinates of the points - (*x*,*y*,*z*)			
O	(0,0,6.1)		
A	(12.57,0,4.55)	A’	(24.38,0,0)
B	(6.285,-10.885,4.55)	B’	(12.9,-21.115,0)
C	(-6.285,-10.885,4.55)	C’	(-12.9,-21.115,0)
D	(-12.57,0,4.55)	D’	(-24.38,0,0)
E	(-6.285,10.885,4.55)	E’	(-12.9,21.115,0)
F	(6.285,10.885,4.55)	F’	(12.9,21.115,0)

A number of researchers have analyzed the dome whose geometry is given in Fig. 3. Detecting the limit point is possible by these methods, but most of the methods eluded the fact that the structure switches between post buckling paths. The frame is restrained against displacement and rotation at supports. A vertical load is applied at the apex (O) , and vertical displacements are measured to obtain the load-displacement response. The system's two different post-limit point paths correspond to two different responses. The first path in which the structure is more stiffer is the one obtained when a notional force is applied at D. The second path is obtained when the structure is acted upon by a pair of equal and opposite forces on A and D. The TL formulation in Section 2, software packages like SAP2000 and ABAQUS can predict both the displacement responses accurately.

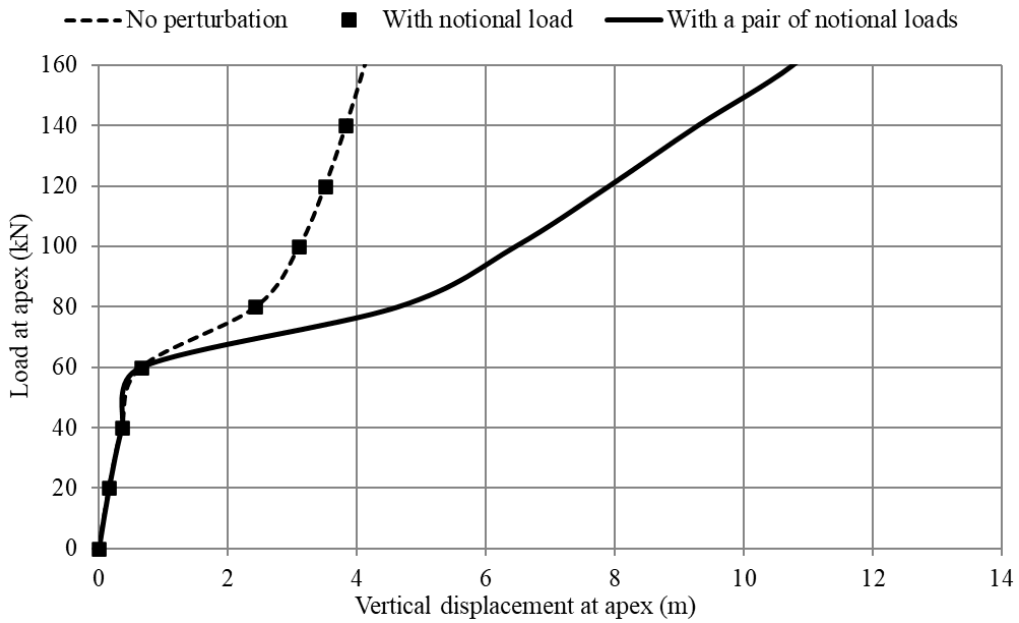

Figure 4: Load-displacement graph for the dome in Fig. 3

The updated Lagrangian (UL) formulation provided by Lip Teh (2004) can identify the branch switching through corrector matrices. From the perspective of a designer opting for DAM, the notional loads should be chosen such that the structure is driven to all the secondary paths possible. For software packages used in this work, perturbation in the form of a force and a couple lead to two different post-buckling paths. If DAM is to be applied for a frame with inclined members (dome), the second-order analysis should not elude the branch switching in the behavior. It should be noted that the methods identified in the literature that elude the second post-buckling path give good results when verified against the two benchmark problems in ANSI/AISC 360-16.

To understand how eluding the rotational mode about a vertical axis through the frame apex will lead to underestimation of design loads, the applicability of DAM and ELM on the frame is discussed. Effective length factor was determined using analysis softwares and alignment charts. Three separate analyses are required and parameters of each model are tabulated in Table 2.

Table 2: Modeling parameters for analysis of hexagonal frame

	Parameter	ELM	DAM	
		Model I	Model II	Model III
Determination of P_u & M_u	Reduced stiffness, E*	E	0.8E	0.8E
	Notional loads	No	One notional load	A pair of equal and opposite notional loads
	Effective length factor (K)	0.748	1	1
Determination of member strength	Nominal compressive strength (P_n) (kN)	190.92	148.49	148.49
	Nominal bending strength (M_n) (kNm)	189.13	189.13	189.13

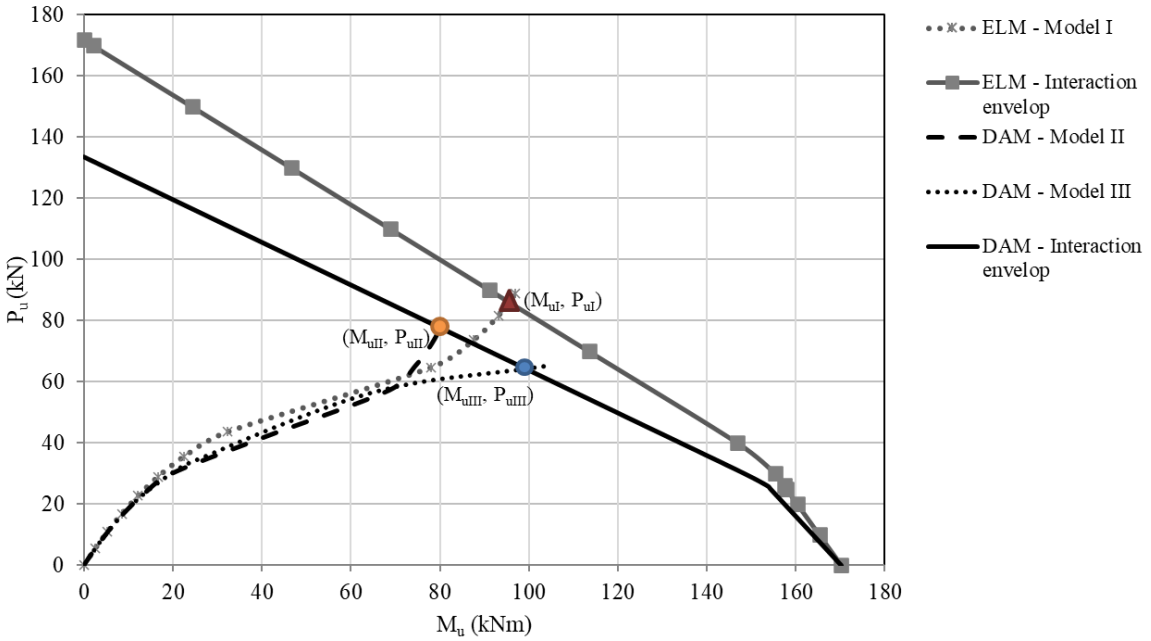

Figure 5: Comparison between design loads predicted by ELM and DAM based on ANSI/AISC 360-16

For models I, II, and III, Fig. 5 shows the intersection of P_u-M_u curves for the inclined member AA' of Fig. 3 with the interaction curves for ELM and DAM. For the model I, P_{uI} and M_{uI} correspond to the second-order member forces in AA' and represent the true response of the structure under applied loads. For model II, P_{uII} and M_{uII} represent the design loads predicted by DAM under a single notional load. In model III, a pair of notional loads are applied, and the design loads are P_{uIII} and M_{uIII}. It is assumed that the member has sufficient yield stress, so that yielding never precedes instability.

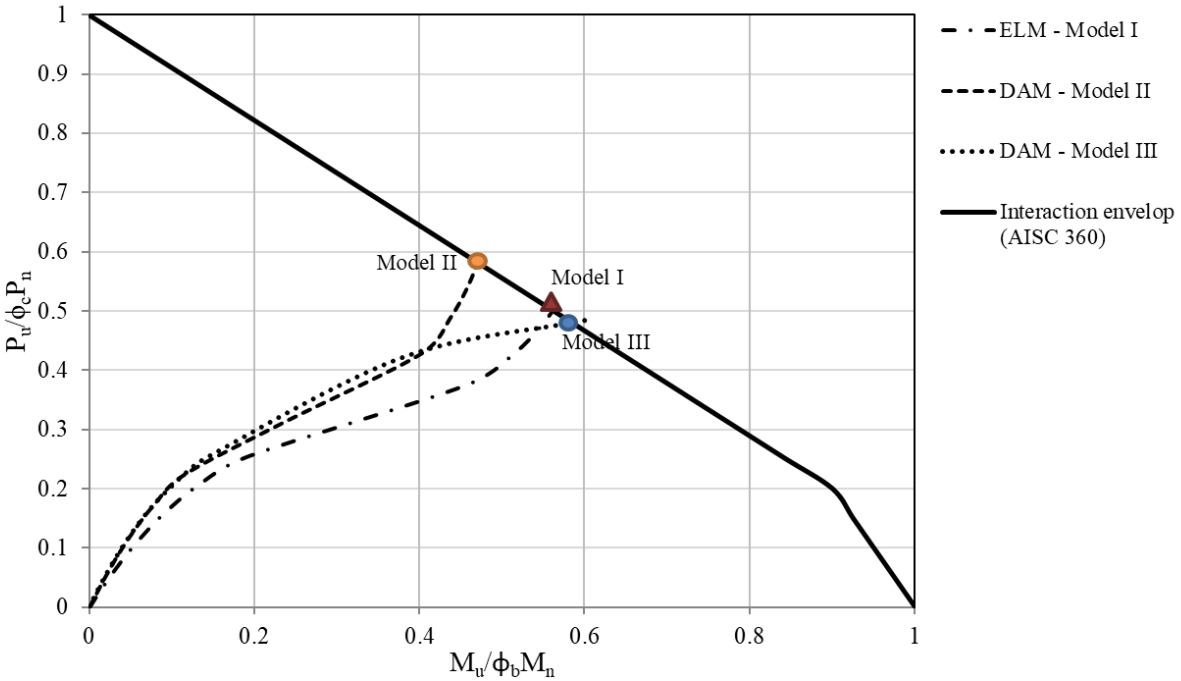

Figure 6: Comparison between design loads predicted by ELM and DAM using non-dimensionalized parameters

In DAM, applying a single notional load predicts second-order moments (M_{uII}) less than that of ELM (M_{uI}). The difference in the design moments between models I, II, and III are significant, but moments calculated by DAM with a pair of notional loads (M_{uIII}) are generally conservative and closer to M_{uI}. The agreement between the analysis results of model I and model III is made clear in the non-dimensionalized interaction curve given in Fig. 6. It should be noted that the denominator P_n in Fig. 6 for models II and III are the same but different from P_n of model I. M_n remains the same for all three models.

If branch switching is unaccounted in the analysis, then DAM will result in design strengths, which are unconservative. In this problem, application of a pair of equal and opposite notional loads in DAM brought out the true behavior of the structural system. Hence, it is suggested that when the behavior is not clearly understood by the designer, application of a few combination of notional loads may be tried by the designer to reveal the entire spectrum of deformation responses of the structure to the applied loads.

3.2 Cable supported beam column

This example may be used as a benchmark problem to ascertain the capabilities of a second-order analysis software for DAM in a system:

(*i*) When highly nonlinear elements like cables support the structure

(*ii*) The structure is lightweight and subjected to lateral force, yet the response is nonlinear

A 2D equivalent beam column model of a guyed mast supported by two cables, as shown in Fig. 7, has been solved using a nonlinear finite element analysis by Schrefler et al.(1983), who modeled the cables and the equivalent beam-column using parabolic line elements. The same problem was solved using SAP2000 and ABAQUS. Fig. 8 compares the load-displacement responses predicted by different nonlinear analyses

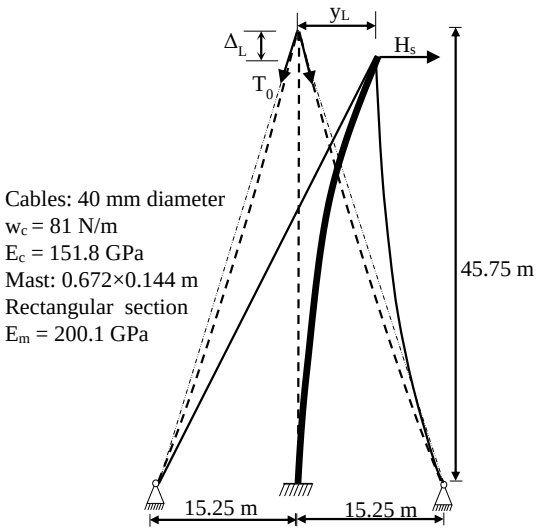

Figure 7: A 2D equivalent beam column model of a guyed mast under lateral load(Schrefler et al. 1983)

. The SAP2000 model uses an in-built nonlinear cable analysis to determine unstretched length. The ABAQUS model uses second-order quadratic hybrid beam elements with 'no compression'

property for cables and quadratic second-order beam elements for the equivalent beam-column. Self-weight of cables was applied as distributed line loads on the beam elements used to discretize the cable. SAP2000 uses a nonlinear large deformation analysis, yet the software fails to capture nonlinearity beyond a specific load (1200 kN). The structure behaves stiffer in SAP2000. The SAP2000 results are helpful when the deflections are small, and even though cables are highly nonlinear elements, the structural response is linear. But, when the deflection is large, the behavior is accurately predicted by ABAQUS.

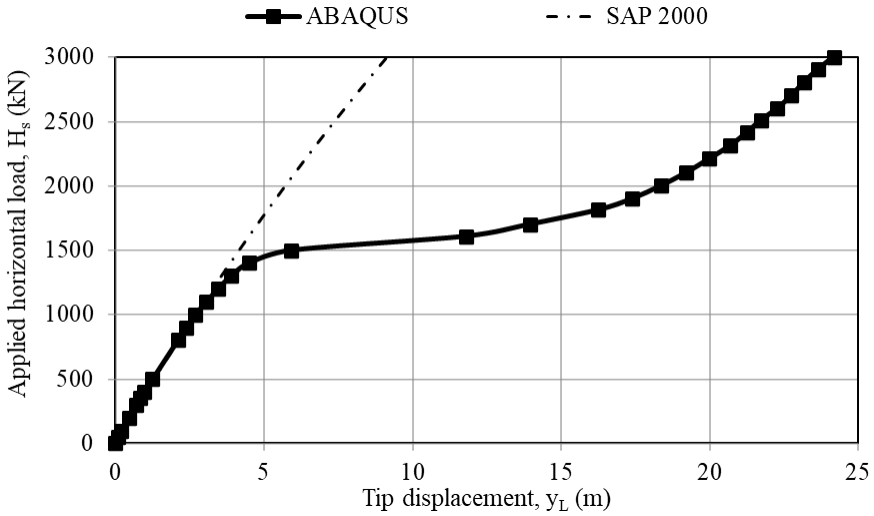

Figure 8: Load-displacement response of guyed mast

A comparison between capabilities of SAP2000 and ABAQUS for benchmark problems available in the ANSI/AISC 360-16 and present study is tabulated in Table 3.

Table 3: Comparison of capabilities of analysis softwares

Source	Benchmark problem	SAP2000	ABAQUS
ANSI/AISC 360-16	Major axis bending of a simply supported column (P – δ effects)	✓	✓
	Major axis bending of a cantilever (P – Δ effects)	✓	✓
Present study	Hexagonal frame (Branch switching)	✓	✓
	Cable supported beam-column (Cable nonlinearity)	☒	✓

The nonlinearity in the structure is by virtue of the large axial load acting on the structure from the cables, even though the external vertical load acting on the structure is zero. If DAM is to be used on cable-supported beam systems, it is essential to ensure that the analysis tool can capture cable nonlinearities even under large displacements. This benchmark example serves this purpose.

4. Conclusions

This paper presents two benchmark problems to ensure that a second-order analysis could capture critical deformation mode for use in DAM. It also discusses the concept of notional loads defined only for gravity-loaded frames with vertical elements in ANSI/AISC 360-16. For 3D structures

with inclined members, the analysis method should accurately capture the spatial behavior, and interaction between bending and twisting of the frame. When the primary buckling mode is not a sway mode, the designer should make appropriate judgments regarding the pattern of notional loads used. If a structure has coincidental or very close buckling modes, structure may switch between modes. The analysis tool used by the designer should be able to accurately capture the entire spectrum of nonlinear post buckling paths. The guidelines in ANSI/AISC 360-16 associate gravity loads acting through out-of-plumbness and bowing of vertical members as the primary source of geometric nonlinearity. A 2D guyed mast with no gravity load is still highly nonlinear owing to the cable behavior and thus might need a rigorous second-order analysis.

Approximate P-Δ and P-δ analyses may be sufficient for use in DAM for simple geometries. But, the generation of benchmark problems needs a rigorous second-order analysis tool to reveal the critical nonlinear behavior under large displacements and rotations. The paper adopts a TL formulation for a 3D beam element. The deformed geometries are modeled using mechanical variables instead of Euler rotation variables, thereby removing the problem of singularity and shear locking, and thus is suited for large displacement analysis of spatial structures. The paper also generates benchmark problems, and the capabilities and a few shortcomings of the widely used nonlinear analysis packages and tools are also discussed from a designer's perspective.

References

ANSI/AISC 360. (2016). *Specification for Structural Steel Buildings*.

Bai, R., Liu, S. W., Liu, Y. P., and Chan, S. L. (2019). "Direct analysis of tapered-I-section columns by one-element-per-member models with the appropriate geometric imperfections." *Engineering Structures*, Elsevier Ltd, 183, 907–921.

Chan, S. L., Liu, Y. P., and Liu, S. W. (2017). "A new codified design theory of second-order direct analysis for steel and composite structures – From research to practice." *Structures*, Elsevier Ltd, 9, 105–111.

Chen, W. F., and Toma, S. (1994). *Advanced analysis of steel frames: Theory, software and applications*. CRC Press, Boca Raton, FL.

Dewobroto, W., and Chendrawan, W. (2018). "Ultimate load capacity analysis of steel scaffoldings Using Direct-Analysis Method." *Practice Periodical on Structural Design and Construction, ASCE*, American Society of Civil Engineers (ASCE), 23(4), 04018028.

Dierlein, G. (2003). *Background and illustrative examples on proposed Direct Analysis Method for stability design of moment frames*. AISC TC 10.

Du, Z. L., Ding, Z. X., Liu, Y. P., and Chan, S. L. (2019). "Advanced flexibility-based beam-column element allowing for shear deformation and initial imperfection for direct analysis." *Engineering Structures*, Elsevier Ltd, 199.

Geschwinder, L. F. (2002). "A practical look at frame analysis, stability and leaning columns." *Engineering Journal, AISC*, 39, 167–181.

Ingkiriwang, Y. G., and Far, H. (2018). "Numerical investigation of the design of single-span steel portal frames using the effective length and direct analysis methods." *Steel Construction*, Ernst und Sohn, 11(3), 184–191.

Liu, S.-W., Bai, R., Chan, S.-L., and Liu, Y.-P. (2016). "Second-order direct analysis of domelike structures consisting of tapered Members with I-sections." *Journal of Structural Engineering*, American Society of Civil Engineers (ASCE), 142(5), 04016009.

Misiunaite, I., and Juozapaitis, A. (2015). "An innovative direct analysis method based approach for the stability control of indirectly supported structures." *Proceedings of the Annual Stability Conference, SSRC*, Nashville, Tennessee.

Pai, P. F. (2007). *Highly flexible structures: Modeling, computation, and experimentation*. *Highly Flexible Structures: Modeling, Computation, and Experimentation*, American Institute of Aeronautics and Astronautics.

Pai, P. F. (2011). "Geometrically exact beam theory without Euler angles." *International Journal of Solids and Structures*, 48(21), 3075–3090.

Schrefler, B., Odorizzis, S., and Woods, R. D. (1983). "A total lagrangian geometrically non-linear analysis of combined beam and cable structures." *Computers & Structures*, 17(I), 115–128.

Shankar Nair, R. (2007). "Stability Analysis and the 2005 AISC Specification." *NASCC: The steel conference*.

Surovek, A. E., and Ziemian, R. D. (2005). “The direct analysis method: Bridging the gap from linear elastic analysis to advanced analysis in steel frame design.” *Proceedings of the Structures Congress and Exposition*, 1197–1210.

Surovek, A., and White, D. W. (2001). “Direct Analysis Approach for the Assessment of Frame Stability: Verification Studies.” *Structural Stability Research Council Annual Stability Conference*, Ft. Lauderdale Fl.

Teh, L. H. (2004). “Beam element verification for 3D elastic steel frame analysis.” *Computers and Structures*, 82(15–16), 1167–1179.

Toma, S., Chen, W.-F., and White, D. W. (1995). “A selection of calibration frames in North America for second-order inelastic analysis.” *Engineering Structures*, 17(2).

Vogel, U. (1985). “Calibrating Frames.” *Stahlbau*, 295–311.

White, D. W., and Hajjar, J. F. (1997). “Design of steel frames without consideration of effective length.” *Engineering Structures*, 19(10), 797.

Ziemian, C. W., and Ziemian, R. D. (2021a). “Efficient geometric nonlinear elastic analysis for design of steel structures: Benchmark studies.” *Journal of Constructional Steel Research*, Elsevier Ltd, 186.

Ziemian, C. W., and Ziemian, R. D. (2021b). “Steel benchmark frames for structural analysis and validation studies: Finite element models and numerical simulation data.” *Data in Brief*, Elsevier Inc., 39.

Ziemian, R. D., Batista Abreu, J. C., Denavit, M. D., and Denavit, T.-J. L. (2018). “Three-dimensional benchmark problems for design by advanced analysis: Impact of twist.” *Journal of Structural Engineering*, American Society of Civil Engineers (ASCE), 144(12), 04018220.